

Cloud Microphysics Retrieval Using S-Band Dual-Polarization Radar Measurements



J. Vivekanandan,* D. S. Zrnic,+ S. M. Ellis,* R. Oye,* A. V. Ryzhkov,+ and J. Straka#

ABSTRACT

Recent studies have shown the utility of polarimetric radar observables and derived fields for discrimination of hydrometeor particle types. Because the values of the radar observables that delineate different particle types overlap and are not sharply defined, the problem is well suited for a fuzzy logic approach. In this preliminary study the authors have developed and implemented a fuzzy logic algorithm for hydrometeor particle identification that is simple and efficient enough to run in real time for operational use. Although there are no in situ measurements available for this particle-type verification, the initial results are encouraging. Plans for further verification and optimization of the algorithm are described.

1. Introduction

The recent deployment of multiparameter, polarimetric radars provides the impetus for development of microphysical retrievals. The primary objective of this paper is to describe a particle classification technique that makes use of polarimetric radar observations. The particle classification technique is computationally simple enough to be implemented for real-time research and operational field programs. Also, when the NEXRAD (Next Generation Weather Radar) is upgraded to dual-polarization capability, operational radar meteorologists might be able to merge kinematic (Doppler data) and microphysical characteristics (polarization radar data) to improve forecasts. One of the merits of the technique described in this paper is that a radar meteorologist may not be required to know the complicated details and the intricacies of interpreting the data associated with polarimetric radar data processing.

Several studies have shown that polarimetric observables (both linear and circular) can be used to identify hydrometeor types (Aydin et al. 1986; Doviak and Zrnic 1993; Hall et al 1984; Hendry and Antar 1984; Lopez and Aubagnac 1997; Straka and Zrnic 1993). Hendry and Antar (1984) used circular polarization measurements for delineating the major precipitation types such as drizzle, rain, melting layer, snowflakes, ice crystals, and ice pellets. However, rain or anisotropic precipitation in the propagation path between the antenna and the radar resolution volume introduces more bias in circular polarization radar measurements than in the case of linear polarization (Doviak and Zrnic 1993). Linear polarimetric radars, like the one used in this study, transmit and receive both horizontally and vertically polarized radiation, providing more information about the scattering media than conventional radar. Polarimetric radar observables depend on the microphysical characteristics of hydrometeors; namely, (a) particle size, (b) particle shape, (c) particle orientation relative to the local vertical direction, (d) phase (liquid or ice), and (e) bulk density (wet, dry, aggregate, or rimed). In addition to traditional reflectivity (Z_{HH}) and Doppler measurements, linear polarimetric observables include differential reflectivity (Z_{DR}), linear depolarization ratio (LDR), specific differential propagation phase (K_{DP}), and correlation coefficient (ρ_{HV}). Reflectivity is related to the power of a horizontally polarized backscattered electric field from a radar resolution

*National Center for Atmospheric Research, Boulder, Colorado; the National Center for Atmospheric Research is partially sponsored by the National Science Foundation.

+National Severe Storms Laboratory, Norman, Oklahoma.

#University of Oklahoma, Norman, Oklahoma.

Corresponding author address: J. Vivekanandan, National Center for Atmospheric Research, P.O. Box 3000, Boulder, CO 80307.
E-mail: vivek@ucar.edu

In final form 17 November 1998.

©1999 American Meteorological Society

volume for a horizontally polarized transmitted wave (copolar). Reflectivity is the sixth moment of the particle size distribution when particle size is small compared to the wavelength. Differential reflectivity is the ratio of the horizontal copolar return to the vertical copolar return and can be interpreted as the reflectivity weighted mean-axis ratio of the precipitation particle in the radar resolution volume (Jameson 1983). Thus, Z_{DR} (in combination with reflectivity) is a good discriminator between oblate rain (high Z_{DR}) and more spherical hail (low Z_{DR}). The rain medium is typically characterized by $Z_{DR} \geq 0.5$ dB and $Z_{HH} \leq 60$ dBZ; and hail by $Z_{DR} \approx 0$ dB or even slightly negative, while Z_{HH} is ≥ 45 dBZ (Aydin et al. 1986; Doviak and Zrnica 1993; Lopez and Aubagnac 1997; Straka and Zrnica 1993). Based on these findings, the anticorrelated pattern between Z_{DR} and reflectivity has been used for hail detection (Aydin et al. 1986; Bringi et al. 1986). Linear depolarization ratio is the ratio between vertically polarized power backscattered for a horizontally polarized transmitted wave and copolar backscattered power. Tumbling, wet nonspherical particles such as hail, melting aggregates, wet graupel, and bright band due to melting (Vivekanandan et al. 1990; Zrnica et al. 1993) are identified with large LDR values whereas light rain, cloud droplets, and dry ice particles are associated with low LDR values. Specific differential propagation phase is the difference in phase per kilometer of the received horizontal and vertical polarized waves. It is almost linearly proportional to rain rate and ice water content (Sachidananda and Zrnica 1986; Vivekanandan et al. 1994). Here, K_{DP} can be used to identify nonspherical particles, such as ice crystals and raindrops. A combination of specific differential phase, reflectivity, and Z_{DR} can be used for inferring rain intensity and mixed-phase characteristics (Balakrishnan and Zrnica 1990). Vivekanandan et al. (1994) describe a method for delineating regions of pristine ice crystal and snow using Z_{HH} and Z_{DR} observations. The correlation coefficient between copolar returns is denoted as ρ_{HV} . Values of ρ_{HV} are close to unity for rain and pure ice crystals. In the case of melting and mixed phase (rain and hail or graupel) conditions, ρ_{HV} is smaller than unity because of the variability in scattering characteristics of precipitation particles for a given size. Low values of ρ_{HV} may be used for detecting hail and mixed phase.

Typical thresholds of polarimetric observables for various precipitation types are listed in Table 8.1 of Doviak and Zrnica (1993). These thresholds are based on model computation and limited comparison of ra-

dar measurements with in situ aircraft and ground observations. Using some of these thresholds, Lopez and Aubagnac (1997) developed an algorithm to identify regions of liquid, frozen (hail and graupel only), and mixed-phase precipitation Z_{HH} and K_{DP} . They then used Z_{HH} and Z_{DR} to differentiate among graupel, small hail, and large hail and to investigate the relations among liquid particles, frozen particles, and lightning frequency in thunderstorms. Straka and Zrnica (1993) proposed a method, also based on the thresholds of Doviak and Zrnica (1993), using Z_{HH} , Z_{DR} , ρ_{HV} , K_{DP} , LDR knowledge of the freezing level in cloud, and electromagnetic scattering models to alleviate ambiguities in hydrometeor types and quantities. It was proposed that accurate microphysical retrievals could improve numerical weather prediction (Sun and Crook 1997). Holler et al. (1994) developed a “semiempirical” hydrometeor discrimination algorithm using thresholds of Z_{DR} and LDR and an estimate of the melting level. They used their method to study the life cycle of hail in a convective storm.

Notice that each of the above-discussed techniques uses thresholds, or hard boundaries to identify particle classes. The use of hard boundaries can lead to misclassification because there is a fair amount of overlap between polarimetric observables for various precipitation types. Boundaries between polarimetric observables are “fuzzy” as shown below.

2. Fuzzy logic method

Probabilistic and fuzzy logic methods share many similarities. Both systems describe uncertainty numerically in the interval between 0 and 1. In a probabilistic method, the intersection between a set and its complement is a null set, but it may not be a null set in the case of a fuzzy logic method. For example, rain and no rain regions might contain mixed phase particles, such as melting ice particles or rain and hail mixtures. Thus, there is fuzziness or a nonempty set between an object and its opposite. Objects or events that exhibit fuzziness are classified as fuzzy sets. Further details on the key differences between probabilistic and fuzzy logic methods are discussed in Kosko (1994). The fuzzy boundaries between polarimetric observables are ideally suited for a fuzzy logic-based particle classification approach. In a fuzzy logic-based approach there is a smooth transition in polarimetric observable boundaries among precipitation types. Figure 1 shows a conceptual model of a

fuzzy logic technique for detecting rain and hail using Z_{HH} , Z_{DR} , and LDR. Membership functions for Z_{HH} , Z_{DR} , and LDR define the boundary between the rain and hail regions and are formulated based on their typical values. For particular values of Z_{HH} , Z_{DR} , and LDR, membership functions determine the degree to which an observation belongs to each of the appropriate fuzzy sets, that is, rain and hail (see Fig. 1). An anticorrelated pattern between Z_{HH} and Z_{DR} for hail is reflected in the membership function curves. Both Z_{HH} and Z_{DR} tend to be higher in heavy rain than light rain. Linear depolarization for hail is greater than the corresponding values for rain regions. Because they allow for varying values of membership, membership functions are more realistic than a single-valued threshold. The shape of membership functions is determined using information obtained from various studies using polarimetric radar model computations (Bringi et al. 1986; Jameson 1983), joint analysis results using aircraft (Doviak and Zrnica 1993; Holler et al. 1994; Vivekanandan et al. 1990; Zrnica et al. 1993), disdrometer (Aydin et al. 1986), and radar measurements (Balakrishnan and Zrnica 1990; Vivekanandan et al. 1994). Since the technique is based on a fuzzy logic method that makes use of the number of input variables, the particle classification might be insensitive to the fine details in the membership functions. The proposed membership functions would be tuned and adjusted as we acquire more polarimetric datasets with in situ observations.

Consider the simplified example illustrated in Fig. 1. Using membership functions to determine the degree to which each input (here, Z_{HH} , Z_{DR} , and LDR) belongs to each fuzzy set (here, rain and hail) is called “fuzzification” of input. Fuzzification results in a number between 0 and 1 for each input corresponding to each of the fuzzy sets. The results of fuzzification (i.e., $P_i^{Z_{HH}}$, $P_i^{Z_{DR}}$, P_i^{LDR}) are multiplied by a predetermined weight (W_j), the value of which is based on the usefulness for particle classification and the measurement accuracy of the input variable. The weighted results of the fuzzification ($P_i^j W_j$) are summed to produce a single value for each of the fuzzy sets Q_i , (i.e., the particles rain and hail). This unification of fuzzy outputs

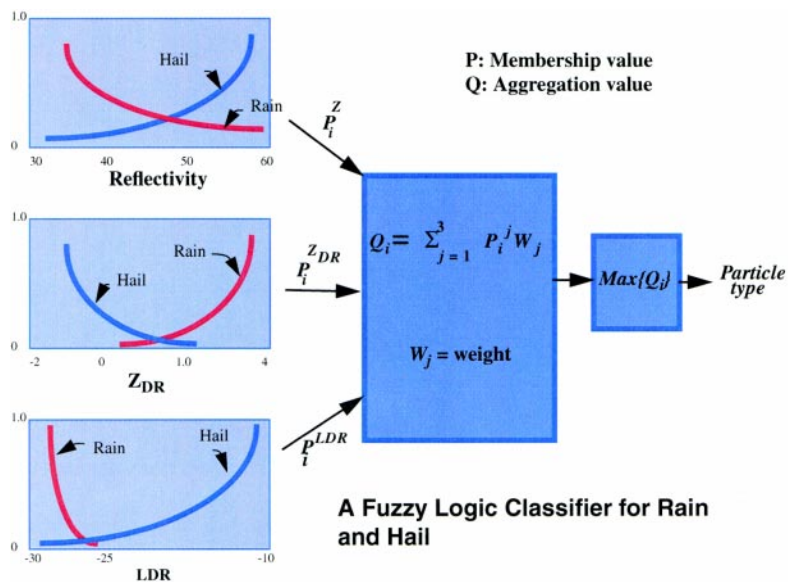


FIG. 1. An example of a fuzzy logic particle identification algorithm. For each variable, all of the particles receive a value between 0 and 1 from the respective membership function (fuzzification). These values (P) are then multiplied by the appropriate weight (W) and summed for each particle. The maximum of the weighted sums is then found to determine the particle type.

for all the fuzzy-set rules is called aggregation. The fuzzy outputs of the aggregation process (Q_i) are then defuzzified using a function that determines the maximum among the fuzzy sets. The fuzzy set with the maximum value is identified as the particle type for the given Z_{HH} , Z_{DR} , and LDR values.

The mathematical operations involved in the above-described fuzzy logic procedure are (i) a lookup table for the membership functions to fuzzify the input, (ii) multiplication and addition for the aggregation procedure, and (iii) finding the maximum among aggregated values for defuzzification, that is, precipitation-type identification. The simplicity and efficiency of the method allows for real-time calculation and display of hydrometeor discrimination. Also, it is straightforward and easily modified for the optimization of particular radars and applications. Classification based on multiple one-dimensional membership functions has been demonstrated by Straka (1996) with examples of hydrometeor fields that conform to accepted conceptual models.

The software used to generate the particle identification can read the real-time radar data from the S-Pol radar (Lutz et al. 1997) and translator routines convert the data into the proper format for processing and display. Each radar resolution volume in the radar space is classified into one of the 15 particle types as shown in Fig. 2. For clarity of presentation and vi-

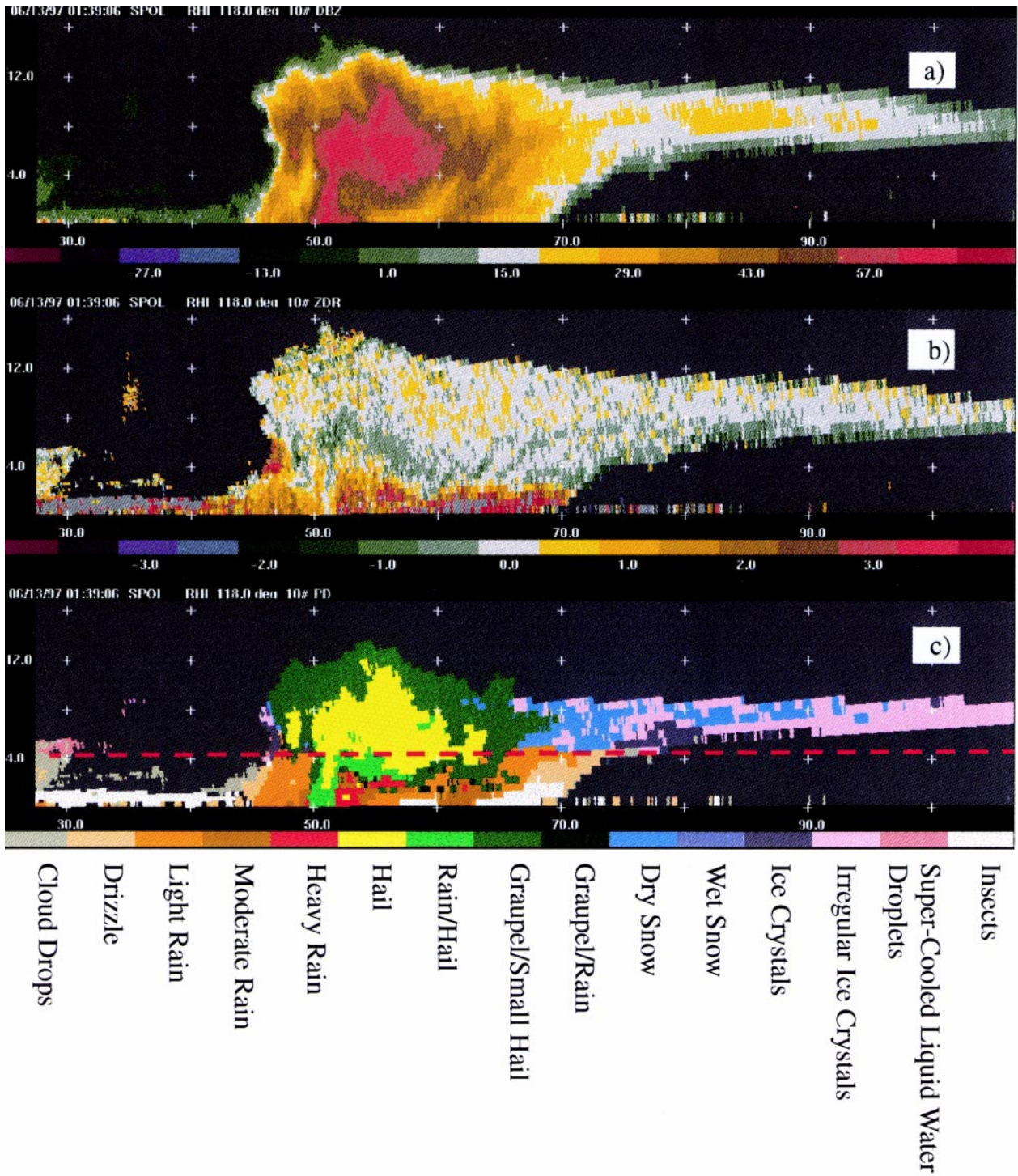


FIG. 2. (a) A plot of reflectivity vs Z_{DR} for regions of liquid drops and hail. The spread in Z_{DR} , due to the variability in drop size distribution, is bounded by black lines. (b) As in Fig. 2a with regions denoting 15 different hydrometer classes in color code. The overlap between particles in the Z, Z_{DR} plane is noteworthy. (c) Two-dimensional membership function in Z_{HH}/K_{DP} space. Boundaries of 15 different hydrometer types are shown.

sualization, each particle type is color coded and the result is displayed in the same format as the radar scan (i.e., RHI, PPI, or surveillance). In the case of a long

propagation path through rain, polarimetric radar measurements (especially at frequencies higher than 3 GHz) are biased by attenuation and differential at-

tenuation due to rain and mixed-phase conditions. Using simple power relationships between K_{DP} and attenuation (Bringi et al. 1990), the bias due to propagation effects in rain can be corrected.

3. Two-dimensional membership function

The most important element in fuzzy logic-based classification is the membership functions. Among all of the radar measurements, reflectivity is the most widely used observation for studying precipitation. Therefore, and because the partition of the planes Z_{HH} and X (where X stands for any of the polarimetric variables such as Z_{DR} , K_{DP} , LDR, and ρ_{HV}) into regions of hydrometeor types is well understood, we have constructed two-dimensional membership functions in this space. The two dimensions are reflectivity and one of the polarimetric variables; the value of the membership function varies between 0 and 1 in the specified region. Boundaries between liquid droplets and hail in the Z_{HH} - Z_{DR} plane are sketched in Fig. 3a. The region bounded by solid black lines corresponds to the range of Z_{DR} values of liquid droplets for a given value of Z_{HH} . Natural variability in raindrop size distribution introduces scatter between Z_{HH} and Z_{DR} (Chandrasekar and Bringi 1988); therefore, there is a fair amount of overlap between Z_{HH} and Z_{DR} values for various rain intensities. Figure 3b shows boundaries for all 15 different precipitation classes using Z_{HH} and Z_{DR} . Figure 3c is similar to Fig. 3b except precipitation boundaries are shown in the Z_{HH} - K_{DP} plane.

To facilitate simpler implementation of membership functions, the two-dimensional functions are decomposed into a multitude of one-dimensional functions as follows. For a given Z_{HH} , the membership function is unity in regions bounded by a polarimetric variable; at the edge of the regions the membership function linearly decreases to zero. Thus, the profile of the membership function for a constant Z_{HH} is a trapezoid bracketing the appropriate values of the polarimetric variable. Trapezoidal membership functions are formulated for every 2-dB increment in reflectivity values of each particle category to generate each of the two-dimensional membership functions of Z_{HH} - Z_{DR} , Z_{HH} - K_{DP} , Z_{HH} -LDR, and Z_{HH} - ρ_{HV} . Reflectivity and temperature (T) membership functions are one-dimensional. Proximity sounding data are used to obtain the temperature profile. The temperature membership function is nonzero only if the

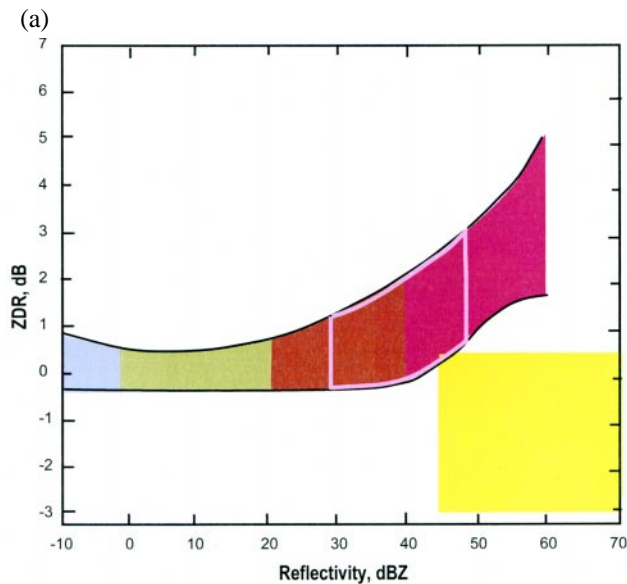
observed reflectivity is within the permissible range of reflectivity for the corresponding particle type.

The six different observations (Z_{HH} , Z_{DR} , K_{DP} , LDR, ρ_{HV} , and T) are fuzzified using the corresponding membership functions. The fuzzification results are multiplied by weights determined subjectively by the general accuracy of the variable and how well the variable indicates different particle types. Currently the weights for Z_{HH} , Z_{DR} , and T are twice the weights for K_{DP} , LDR, and ρ_{HV} ; however, we plan to optimize the weights as we gain experience with the algorithm. The six weighted results of the fuzzification are summed to produce a single aggregated value for each of the 15 particle types. The particle type with the maximum aggregated value is identified as the dominant particle type for the given Z_{HH} , Z_{DR} , K_{DP} , LDR, ρ_{HV} , and T observation.

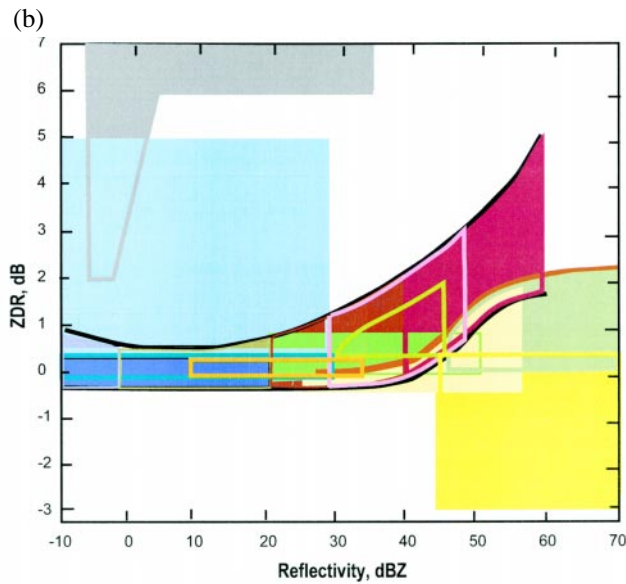
4. Results of particle classification

In the spring of 1997, S-Pol was deployed near Wichita, Kansas, as part of the Cooperative Atmospheric Surface Exchange Study (CASES-97). The experiment was performed to study the exchange of energy, moisture, polarimetric radar-based precipitation estimation, and trace chemicals between the land and atmosphere in the Walnut Creek watershed in Kansas (LeMone et al. 1998). On 13 June 1997, S-Pol recorded data of a severe thunderstorm to the east of the radar. RHI scans of Z_{HH} , Z_{DR} , and the corresponding particle classification results are shown in Figs. 2a-c, respectively. The storm extends to 16 km in height and has a well-defined anvil, an overshooting top, and a weak echo region. The storm persisted for 90 min beyond the time of the RHI's shown in Fig. 2.

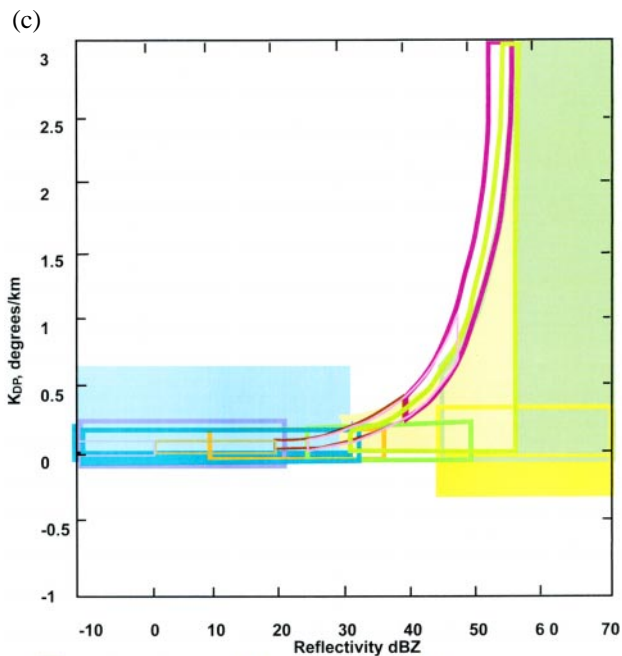
The spatial variation in Z_{HH} and Z_{DR} shown in Fig. 2 suggests the existence of a variety of particle types. As expected, the high reflectivity and low Z_{DR} regions are classified as hail by the fuzzy logic-based technique (Fig. 2c). There were reports of large hail associated with this cell near the time of the observation filed by the National Weather Service. However, no in-cloud aircraft measurements were available for verification. Regions with moderate reflectivity and $Z_{DR} > 0.5$ dB were identified as light (< 10 mm h^{-1}), moderate (< 40 mm h^{-1}), and heavy (> 40 mm h^{-1}) rain intensities. Rain-hail and graupel-rain mixed precipitation types were detected below hail regions and above rain regions. This is gratifying since raindrops



cloud drops
drizzle
light rain
moderate rain
heavy rain
hail



cloud drops
drizzle
light rain
moderate rain
heavy rain
hail
rain/hail
graupel/small hail
graupel/rain
dry snow
wet snow
ice crystals
irregular ice crystals
supercooled liquid droplets
insects



cloud drops
drizzle
light rain
moderate rain
heavy rain
hail
rain/hail
graupel/small hail
graupel/rain
dry snow
wet snow
ice crystals
irregular ice crystals
supercooled liquid droplets
insects

may be produced by hail–graupel melting as it descends, along with water-shedding processes. Also, hail has a higher fall speed than raindrops and may fall through regions of rain. Graupel–small hail was identified just above the hail region. Above freezing level, the low reflectivity (< 30 dBZ) pixels were clas-

FIG. 3. RHI scans of (a) Z_{HH} , (b) Z_{DR} , and (c) the corresponding particle classification results (the dashed line denotes the freezing level). The radar measurements were collected by the NCAR S-Pol radar during the CASES-97 field program.

sified as dry snow, irregular ice crystals, ice crystals, or supercooled liquid droplets. These small ice particles are found mostly in the anvil and near the top of the storm as would be expected. Below the freezing level, low reflectivity values were classified as drizzle or cloud drops. It is noteworthy that a layer of high Z_{DR} (> 5 dB), with a low-reflectivity region to the left of the precipitation echo, is classified as insects (Wilson et al. 1994).

5. Conclusions

The fuzzy logic–based method described above makes use of a smooth transition in polarimetric observable boundaries among precipitation types instead of simple thresholds. The mathematical operations involved are simple, linear, algebraic operations, and, hence, the particle classification procedure can be implemented for real-time applications. Also, the method is robust enough that its performance may not be adversely affected due to typical measurement error in some of the input variables. Alternate methods such as the statistical decision theory method and neu-

ral network approach are not feasible at the moment because of the limitation on in situ microphysical precipitation data in conjunction with polarization radar measurements. The lack of in situ microphysical data is a limiting factor for training neural networks and also for obtaining the required statistical decision theory-based approaches. Results of the fuzzy logic-based particle classification approach show important aspects of the microphysical structure of a typical convective thunderstorm. The boundaries between various precipitation types are defined using reflectivity and polarimetric radar observables. Even though reflectivity, Z_{DR} and temperature profile play an important role in particle identification, the other polarimetric variables are needed for classifying mixed-phase precipitation.

Quantification of the precipitation amounts can be improved using the results of particle classification. Power-law relationships that are used for precipitation estimation can be modified based on particle type to obtain better accuracy. Also, assimilation of radar-derived cloud microphysics into cloud models will improve the initial conditions of a numerical storm forecast (Sun and Crook 1997). The particle-type identification program has been incorporated into the S-Pol radar precipitation product package and displays the results in real time. We plan to verify and improve the particle classification technique using observations collected by cloud physics aircraft during the Florida component of TRMM/Texas and Florida Underflights (TEFLUN-B). We envision that particle classification would also identify convective and stratiform regions in clouds. The separation of cloud systems into convective and stratiform is one of the primary objectives of TRMM for obtaining four-dimensional structures of latent heating in the atmosphere (Simpson 1988).

Acknowledgments. This research is sponsored by the National Science Foundation through an Interagency Agreement in response to requirements and funding by the Federal Aviation Administration's Aviation Weather Development Program. The views expressed are those of the authors and do not necessarily represent the official policy or position of the U.S. government.

References

Aydin, K., T. A. Seliga, and V. Balaji, 1986: Remote sensing of hail with a dual-linear polarization radar. *J. Climate Appl. Meteor.*, **25**, 1475–1484.

Balakrishnan, N., and D. S. Zrnice, 1990: Estimation of rain and hail rates in mixed-phase precipitation. *J. Atmos. Sci.*, **47**, 565–583.

Bringi, V. N., J. Vivekanandan, and J. D. Tuttle, 1986: Multiparameter radar measurements in Colorado convective storms. Part II: Hail detection studies. *J. Atmos. Sci.*, **43**, 2564–2577.

———, V. Chandrasekar, N. Balakrishnan, and D. S. Zrnice, 1990: An examination of propagation effects on radar measurements at microwave frequencies. *J. Atmos. Oceanic Technol.*, **7**, 829–840.

Chandrasekar, V., and V. N. Bringi, 1988: Error structure of multiparameter radar and surface measurements of rainfall. Part I: Differential reflectivity. *J. Atmos. Oceanic Technol.*, **5**, 783–802.

Doviak, R. J., and D. S. Zrnice, 1993: *Doppler Radar and Weather Observations*. Academic Press, 562 pp.

Hall, M. P. M., J. W. F. Goddard, and S. M. Cherry, 1984: Identification of hydrometeors and other targets by dual-polarization radar. *Radio Sci.*, **19**, 132–140.

Hendry, A., and Y. M. M. Antar, 1984: Precipitation particle identification with centimeter wavelength dual-polarization radar. *Radio Sci.*, **19**, 115–122.

Holler, H., V. N. Bringi, J. Hubbert, M. Hagen, and P. F. Meischner, 1994: Life cycle and precipitation formation in a hybrid-type hailstorm revealed by polarimetric and Doppler radar measurements. *J. Atmos. Sci.*, **51**, 2500–2522.

Jameson, A. R., 1983: Microphysical interpretation of multiparameter radar measurements in rain. Part I: Interpretation of polarization measurements and estimation of raindrop shapes. *J. Atmos. Sci.*, **40**, 1792–1802.

Kosko, B., 1994: *Neural Networks and Fuzzy Systems: A Dynamical Systems Approach to Machine Intelligence*. Prentice-Hall, 449 pp.

LeMone, M. A., and Coauthors, 1998: CASES-98: Diurnal variation of the fair-weather PBL. Preprints, *Special Symp. on Hydrology*, Phoenix, AZ, Amer. Meteor. Soc., 88–92.

Lopez, R. E., and J. P. Aubagnac, 1997: The lightning activity of a hailstorm as a function of changes in its microphysical characteristics inferred from polarimetric radar observations. *J. Geophys. Res.*, **102**, 16 799–16 813.

Lutz, J., B. Rilling, J. Wilson, T. Weckwerth, and J. Vivekanandan, 1997: S-Pol after three operational deployments, technical performance, siting experiences, and some data examples. Preprints, *28th Conf. on Radar Meteorology*, Austin, TX, Amer. Meteor. Soc., 286–287.

Sachidanada, M., and D. S. Zrnice, 1986: Differential propagation phase shift and rainfall rate estimation. *Radio Sci.*, **21**, 235–247.

Simpson, J., R. F. Adler, and G. R. North, 1988: A proposed tropical rainfall monitoring mission (TRMM) satellite. *Bull. Amer. Meteor. Soc.*, **69**, 228–295.

Straka, J. M., 1996: Hydrometeor fields in a supercell storm as deduced from dual-polarization radar. Preprints, *18th Conf. on Severe Local Storms*, San Francisco, CA, Amer. Meteor. Soc., 551–554.

———, and D. S. Zrnice, 1993: An algorithm to deduce hydrometeor types and contents from multiparameter radar data. Preprints, *26th Int. Conf. on Radar Meteorology*, Norman, OK, Amer. Meteor. Soc., 513–515.

Sun, J., and N. A. Crook, 1997: Dynamical and microphysical retrieval from Doppler radar observations using cloud model and its adjoint: Part I. Model developments and simulated data experiments. *J. Atmos. Sci.*, **54**, 1642–1661.

- Vivekanandan, J., V. N. Bringi, and R. Raghavan, 1990: Multi-parameter radar modeling and observations of melting ice. *J. Atmos. Sci.*, **47**, 549–564.
- , ——, M. Hagen, and P. Meischner, 1994: Polarimetric radar studies of atmospheric ice particles. *IEEE Trans. Geosci. Remote Sens.*, **32**, 1–10.
- Wilson, J. W., T. M. Weckwerth, J. Vivekanandan, and R. M. Wakimoto, R. W. Russell, 1994: Boundary layer clear-air radar echoes: Origin of echoes and accuracy of derived winds. *J. Atmos. Sci.*, **51**, 1184–1206.
- Zrnich, D. S., N. Balakrishnan, C. L. Ziegler, V. N. Bringi, K. Aydin, and T. Matejka, 1993: Polarimetric signatures in the stratiform region of a mesoscale convective system. *J. Appl. Meteor.*, **32**, 678–693.

